Supplementary Information

A Novel Electroless Method for the Deposition of Single-Crystalline Gold Nanocrystals On and Inside an Organic Solid-Matrix

Khaleda Banu,†, ‡,* and Takayoshi Shimura§

†Venture Business Laboratory, Center for Advanced Science and Innovation, Osaka University, Suita, Osaka 565-0871, Japan

‡Department of Electrical & Computer Engineering, University of California, SanDiego, 9500 Gilman Drive, La Jolla, San Diego, CA 92093-0407

§Department of Material & Life Science, Division of Advanced Science and Biotechnology, Graduate School of Engineering, Osaka University, Japan

∗Corresponding author's E-mail: kbanu@ece.ucsd.edu, kbanu05@yahoo.com
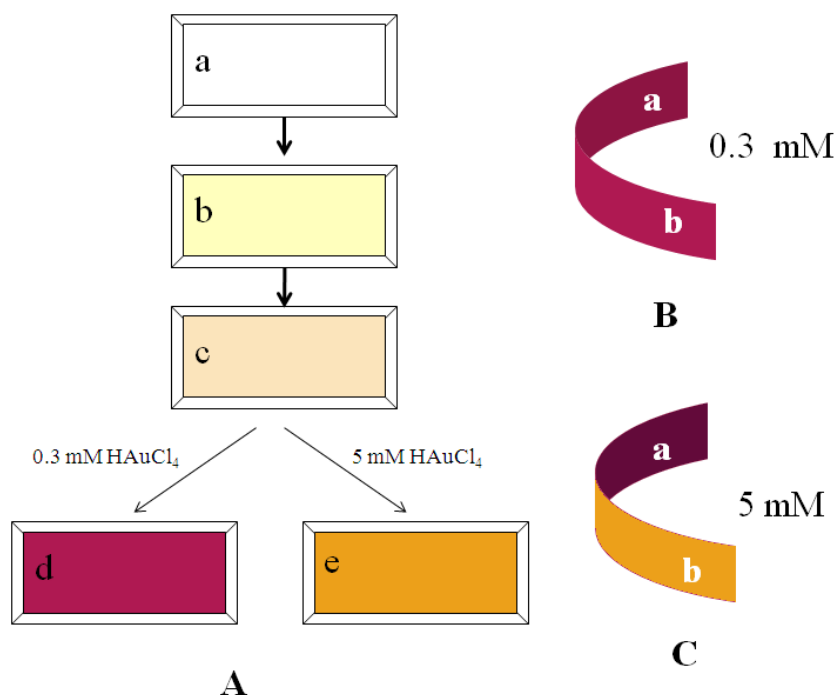
Phone: +1-858-822-4629

Fig. S1 (A) SM Preparation scheme. (a) Clean glass surface, (b) epoxy-thiol coated glass substrate, (c) tannin immobilized epoxy-thiol coated solid matrix, SM, and (d and e) deposition of gold nanoparticles on and inside the SM when the concentration of $HAuCl_4$ in the aqueous phase is 0.3 mM (d) and 5 mM (e).

(B and C) Pictorial presentations of gold-deposited solid matrices (Au-SM) separated from the glass substrate in A(d) and A(e), respectively. Side (a) was attached to the glass surface and was not in contact with the solution during the reaction period. Side (b) was always in contact with the solution during the period of reaction.

(B) Solid matrix from A(d) separated from the substrate after gold deposition. (a) The deep ruby-red color of the SM was observed on both the opposite side (a) and the solution side (b).

(C) The solid matrix from A(e) after gold deposition. (a) The deep ruby-red coloration of the SM observed from the opposite side (a) and the deep golden color from the solution side (b).
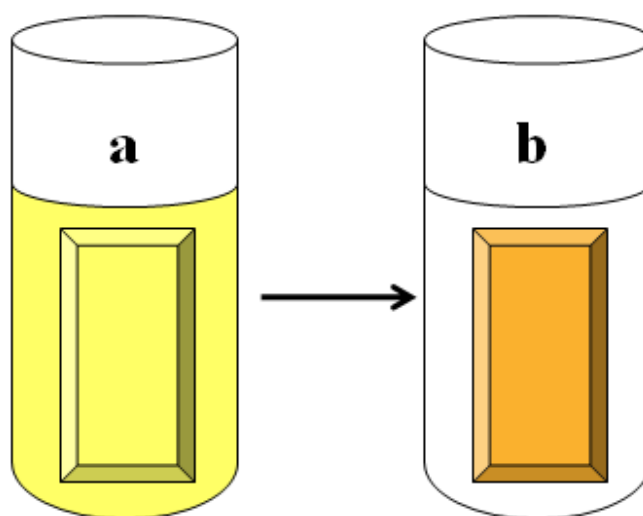
Fig. S2 Simple experimental technique for the deposition of gold single-crystals on and inside the SM. (a) Insertion of SM in 5 mM HAuCl$_4$ at 60 ^{o}C and pH 1. (b) Deposition of single-crystalline gold nanocrystals on and inside the solid matrix after 24 hrs of heating.

Fig. S3 CLS microscope image of the large amount of gold nanosheets deposited on the solution-side of the SM.
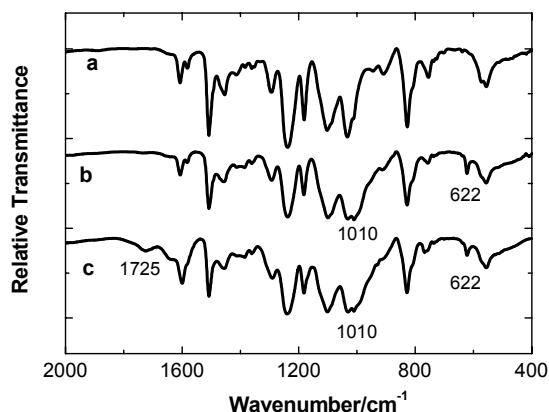
Fig. S4 FTIR-ATR spectra of the solid matrix: (a) epoxy-thiol coated glass substrate, (b) after deposition of gold on the epoxy-thiol coated glass substrate and (c) after the deposition of gold on the tannin-immobilized epoxy-thiol coated solid matrix, SM.

Three new absorption bands, with peaks at 622 cm^{-1}, 1010 cm^{-1} and 1725 cm^{-1} were observed after the reduction of $HAuCl_4$ to metallic gold on and inside the SM (c). In a blank experiment, gold was deposited on and inside an epoxy-thiol coated glass substrate. The peaks at 622 cm^{-1} and 1010 cm^{-1} appeared (b). However, the peak at 1725 cm^{-1} was absent. The peak at 1725 cm^{-1} confirmed the presence of carbonyl functional groups on the SM because of the reduction of the hydroxyl groups of tannin molecules on the solid matrix. However, the peaks at 622 cm^{-1} and 1010 cm^{-1} are associated with the oxidation of thiol derivatives on the SM. The peak at 622 cm^{-1} is due to ring vibration of the thiirane compound generated after the reduction of $HAuCl_4$ to metallic gold.[1] The peak at 1010 cm^{-1} is due to the vibration of sulfoxyl (S=O) groups generated on the SM by the oxidation of thiol derivatives. Therefore, it was confirmed that both tannin and thiol derivatives on the SM interacted with $HAuCl_4$ and played a role in the deposition of gold particles on and inside the solid matrix.[2]
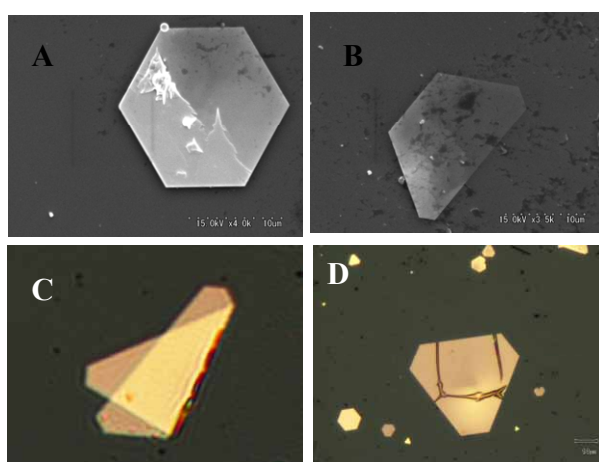
Fig. S5 (A and B) SEM images of transparent nanosheets on the SM. The initially deposited nanoparticles were easily observed through the transparent upper nanosheets. (A and B) Optical microscope images of pinkish-golden nanosheets deposited on the SM (C and D). The folded edge of C was clearly visible through the upper part. Truncated nanosheet with a folded surface (D). The concentration of $HAuCl_4$ was 5 mM, and the deposition proceeded for 5 hrs.
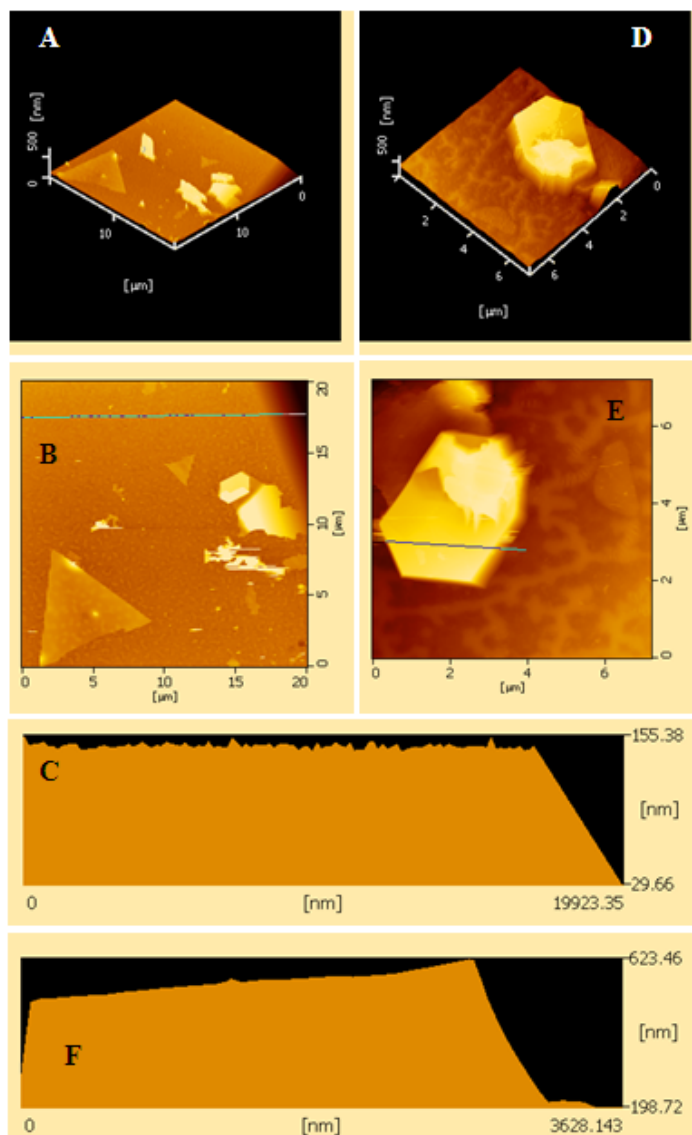
Fig. S6 Atomic force microscopy images of the gold nanosheets on the SM. (A, B) Deposition of a few nanosheets on a large (more than 20 μm) nanosheet. (C) The height of the large nanosheet displayed in (A and B). (D, E) Image of a small nanosheet deposited on the SM (~ 4 μm). (F) The height of the small nanosheet displayed in (D and E).

Supplementary information S7

Estimation of the particle size from the broadening of the XRD reflections by means of the so-called Scherrer formula.

The Scherrer formula is

$$d = \frac{0.9K\lambda}{w \ \cos \theta}$$

where d is the particle size, λ is the wavelength of the radiation in nm, θ is the angle of the Bragg reflection, w is the full width at half-maximum (fwhm) of a particular reflection of interest (in radians), and K is a constant called the shape factor, which takes a value close to 0.89. A constant (0.9) was added to the numerator of the equation, as a Gaussian function (rather than a triangle function) was used to describe the peak. The Scherrer equation can predict the thickness of crystals smaller than 100 nm.

Table 1

Effective crystallite sizes calculated by the Scherrer equation from X-ray diffraction from gold nanocrystals deposited on the opposite side of the SM (data from Figure 5B).

{111} direction (nm)	{200} direction (nm)	{220} direction (nm)	{311} direction (nm)
22.4	12.5	12.3	11.1

The Scherrer formula, based on the full-width at half maximum of different diffraction peaks, gave the different crystallite values shown in Table 1. This calculation showed that the particles on the opposite side of the SM were not spherical and exhibited a sheet morphology.
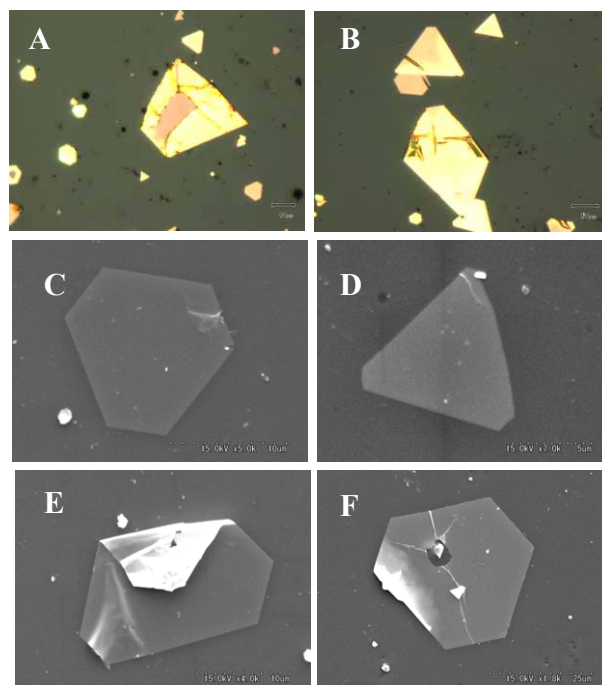
Fig. S8 Optical microscope (A and B) and SEM (C, D, E and F) images of the transparent gold nanosheets deposited on the SM after sonication and washing. Figures A and B show the folded gold nanosheet after washing. Larger sheets were folded much. However, the smaller nanosheets remained completely attached to the surface without folding. The SEM images also confirm that the nanosheets remained on the SM after washing (C, D, E and F). Folded (E) and broken (F) nanosheets were also observed in the SEM measurements.

In addition to the nanosheets, nanoparticles were also present on the SM. This result shows that nanoparticles and nanosheets remained on the SM and did not detach from the surface. The absorption measurements of the SM were also unchanged by washing.
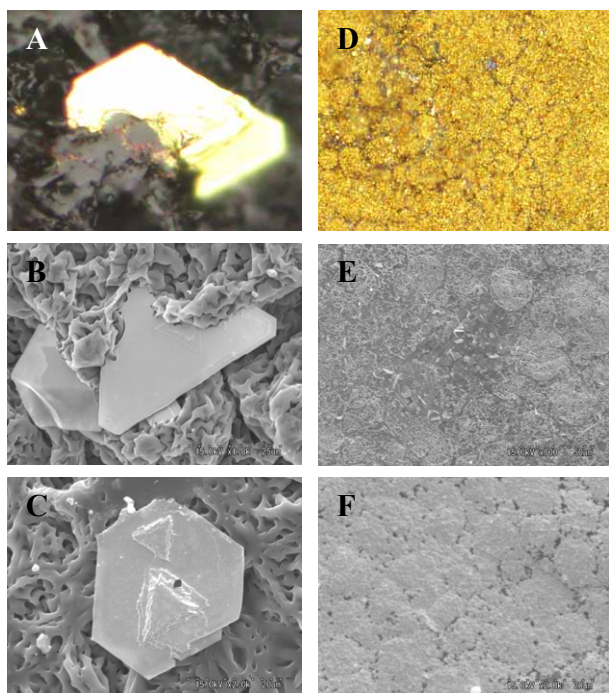
Fig. S9 Optical microscope (A) and SEM (B and C) images of gold nanosheets together with nanoparticles deposited on the SM cured by aliphatic diamine. Optical microscope (D) and SEM (E and F) image of gold nanoparticles deposited on the SM for the epoxy system cured by heterocyclic diamine.

References

1) P. V. Berkel, W. Driessen, J. Reedijk, D. Sherrington and A. Zitsmanis, *Reactive & Functional Polymers*, 1995, **27**, 15.

2) W. Petz, *Coordination Chemistry Reviews*, 2008, **252**, 1689.